35th Annual International Conference of the IEEE EMBS
Osaka, Japan, 3 - 7 July, 2013

Estimating the Center of Mass of a Free-Floating Body in Microgravity

L. Lejeune, C. Casellato, N.Pattyn, X. Neyt, P-F. Migeotte

***Abstract*— This paper addresses the issue of estimating the position of the center of mass (CoM) of a free-floating object of unknown mass distribution in microgravity using a stereoscopic imaging system. The method presented here is applied to an object of known mass distribution for validation purposes. In the context of a study of 3-dimensional ballistocardiography in microgravity, and the elaboration of a physical model of the cardiovascular adaptation to weightlessness, the hypothesis that the fluid shift towards the head of astronauts induces a significant shift of their CoM needs to be tested. The experiments were conducted during the 57th parabolic flight campaign of the European Space Agency (ESA). At the beginning of the microgravity phase, the object was given an initial translational and rotational velocity. A 3D point cloud corresponding to the object was then generated, to which a motion-based method inspired by rigid body physics was applied. Through simulations, the effects of the centroid-to-CoM distance and the number of frames of the sequence are investigated. In experimental conditions, considering the important residual accelerations of the airplane during the microgravity phases, CoM estimation errors (16 to 76mm) were consistent with simulations. Overall, our results suggest that the method has a good potential for its later generalization to a free-floating human body in a weightless environment.**

I. Introduction

Microgravity provides weightless conditions where, according to rigid body physics, the movement of an object is composed only of a translation and a rotation around its center of mass (CoM), both of constant velocity. A motion-based method is proposed which estimates the position of the CoM of a free-floating object using a stereoscopic apparatus. For validation purposes, experimental data were gathered in parabolic flight using a box-like object of known geometry and mass distribution.

This paper constitutes a proof of concept for an application to human subjects in microgravity, as a contribution to the development of a physical model of the cardiovascular system for ballistocardiography signal analyses. Ballistocardiography consists in measuring the acceleration of the human body at the CoM due to cardiovascular activity. The common procedure is to place an accelerometer at the lower-back of the subject by assuming that it is close to the actual CoM. This non-null distance generates artifacts that need to be corrected. Microgravity conditions allows the acceleration to be measured along the 3 dimensions and provides additional information compared to classical on-ground measurements[1]. However, it raises the problem of having the CoM shifted upwards due to a decrease in the fluid concentration gradient inside the body[2].

Research supported by the Belgian Federal Science Policy Office (BELSPO) via the European Space Agency PRODEX program.

L. Lejeune, N. Pattyn, P-F. Migeotte and X. Neyt are with the Vital Signs and Performance (VIPER) research unit of the Royal Military Academy, Brussels, Belgium (email: laurent.lejeune@elec.rma.ac.be).

Claudia Casellato is with the NearLab of the Politecnico di Milano, Italy. (email: claudia.casellato@mail.polimi.it)

II. Protocols and Experimental Procedures

The experiment was performed during the European Space Agency (ESA) 57th parabolic flight campaign in October 2011. The box-shaped object that was manipulated is shown in figure Its dimensions are $800 \times 200 \times 200\,mm$. Fiducial markers have been placed along its edges to improve the robustness of the estimation method. The experiment was conducted by two operators strapped to the floor of the airplane. At the beginning of the parabola, the first operator was standing in front of the cameras holding the object in his hands. At the start of the microgravity phase, which lasts $\sim 20s$, an initial rotation was given to the object. It was then left free-floating as long as possible. A second operator, standing behind the cameras, triggered them using a remote control. Both cameras shot the scene simultaneously at a frame rate of $5fps$. At the end of the parabola, the object was recovered by the first operator. The procedure was repeated several times.

Fig. 1. Object free-floating during a parabola.

III. Methods

The stereoscopic system was calibrated off-line using the CALtag self-identifying checkerboard [3], combined with a MATLAB implementation of Zhang's calibration algorithm [4]. Figure 2 shows the general framework for the data processing stage. Extracting points of interest on the object

is done in a semi-automatic way: For each left/right pair of frames, points were selected manually in the left view. The corresponding point was then found in the right view via epipolar geometry and a simple cross-correlation based method. By triangulating the corresponding 2D points, the depth is reconstructed. The position of the CoM was then estimated using two methods. The first one (leftmost branch) is based solely on geometrical properties and requires the 3D coordinates of at least three corners of a face. A single pair of frames is needed to reconstruct the CoM. The second method, because it relies on motion, needs several consecutive pair of frames to operate. The two methods are presented in more details in the following section.

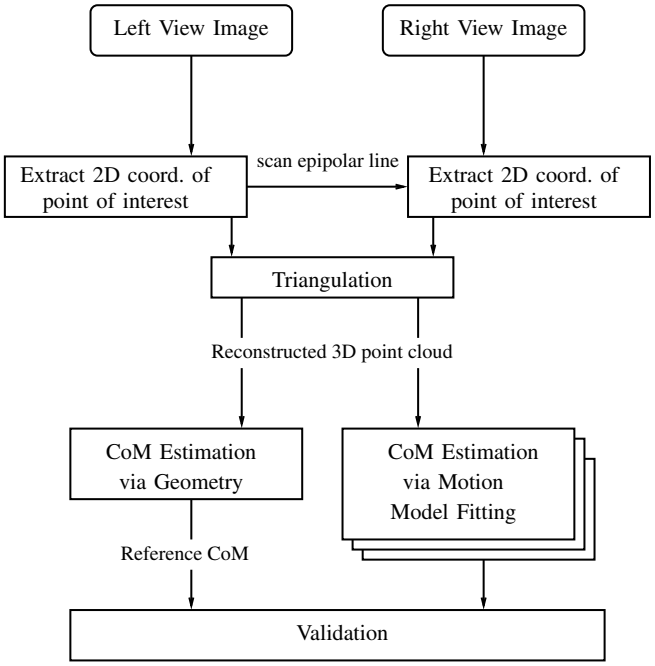

Fig. 2. Framework for the validation of the motion-based method.

A. Geometry-based method

As stated previously, this method only applies for objects of which the geometry and mass distribution is known, providing reference data with which our motion-based method is evaluated. Determining geometrically the position of the CoM of our object is quite straightforward. Given the coordinates of three corners belonging to the same face M_0, M_1 and M_2, the CoM B is calculated using the face center point M_c and the unitary vector $\boldsymbol{n}$ normal to the considered face (cf. figure 3).

$$\boldsymbol{B} = \boldsymbol{M_c} + \frac{l}{2}\boldsymbol{n}$$

B. Motion-based method

This method can be applied in the general case where the mass distribution and the geometry of the object is unknown. However, as will be shown later, a symmetry plane must be defined for the problem to be solvable. The forward model, which given a point-cloud corresponding to a rigid object and a trajectory (translation and rotation), allows to calculate the coordinates of the point-cloud at later time instants. The goal is then to solve the inverse problem, which can be formulated as follows: Assuming that the motion is governed by the proposed forward model and knowing the coordinates of the point-cloud at several time instants, what is the best estimate of the position of the CoM.

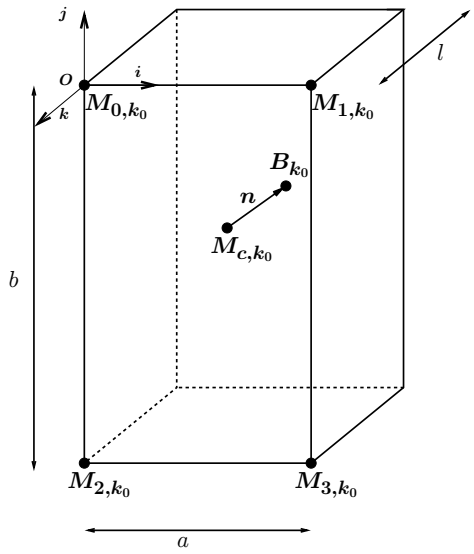

Fig. 3. Box-like object. Four corners are extracted

1) Forward model: It is assumed that the object is observed in an inertial reference frame. Also, the object is rigid and free-floating, i.e. no external force is applied. According to rigid-body dynamics, its movement is composed of a constant translational velocity and a rotation of constant velocity around its CoM. The 3D N-point cloud at time k is written $\{\boldsymbol{M}_{1,k}, ..., \boldsymbol{M}_{N,k}\}$. The associated CoM is denoted $\boldsymbol{B}_k$. The motion depends on the instantaneous translational velocity $\boldsymbol{V}_k$ and rotational velocity $\boldsymbol{\Omega}_k$ which will be referred to by its rotation matrix $\boldsymbol{R}_k$. In order to improve readability, both the translational and rotational velocities are normalized with respect to the sampling period. The coordinate of the CoM at time k is obtained by translating the CoM at time $k-1$ with vector $\boldsymbol{V}_{k-1}$ (eq. 1). The ith point at time $k+1$ $\boldsymbol{M}_{i,k+1}$ is calculated recursively (eq. 2) and a uniform noise $\boldsymbol{w}$ is added that accounts for pixel detection error. is added to the generated point 3.

$$\boldsymbol{B}_k = \boldsymbol{B}_{k-1} + \boldsymbol{V}_{k-1} \tag{1}$$

$$\boldsymbol{M}_{i,k+1} = \boldsymbol{R}_k \left[\boldsymbol{M}_{i,k} - \boldsymbol{B}_k\right] + \boldsymbol{B}_k + \boldsymbol{V}_k \tag{2}$$

$$\tilde{\boldsymbol{M}}_{i,k+1} = \boldsymbol{M}_{i,k+1} + \boldsymbol{w} \tag{3}$$

Figure 4 illustrates a box-shaped object to which our forward model is applied on two consecutive frames.

2) Inverse problem and proof of undeterminacy: The inverse problem consists in estimating $\boldsymbol{B}_{k_0}$ from $\{\tilde{\boldsymbol{M}}_{1,k}, ..., \tilde{\boldsymbol{M}}_{N,k}\}$, $k \in [k_0-\tau; k_0+\tau]$. As stated previously, the inverse problem, due to the property of the rotation operator, is ill-posed. Without loss of generality, let's assume

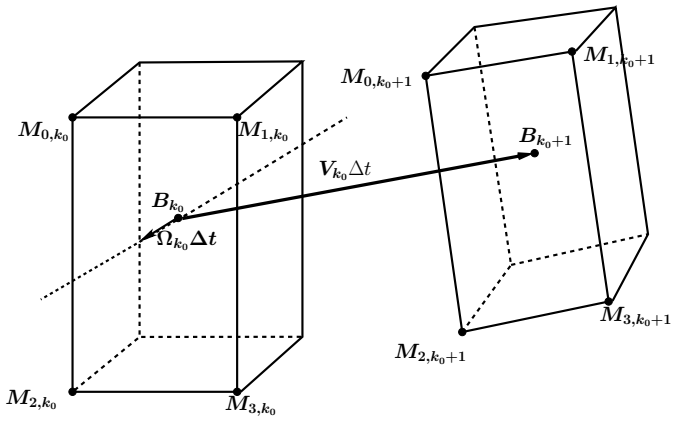

Fig. 4. Applying the forward model to an object.

for now that $\boldsymbol{V}_k = 0$, $\forall k$ and $\hat{\boldsymbol{R}}_k$, the estimate of the rotational velocity, is known. The position of the CoM, which is such that $d\left(\boldsymbol{M}_{i,k_0}, \boldsymbol{B}_{k_0}\right) = d\left(\boldsymbol{M}_{i,k_0+1}, \boldsymbol{B}_{k_0}\right) \quad \forall i$, describes the instantaneous axis of rotation. To circumvent this indeterminacy, one needs to provide a constraint. In our application, because the mass distribution of the considered object is symmetrical, the CoM is contained on a symmetry plane. The CoM will thus be defined as the intersection of the instantaneous axis of rotation with the symmetry plane. In what follows, estimation methods for the motion parameters $\boldsymbol{R}$ and $\boldsymbol{V}$ are presented.

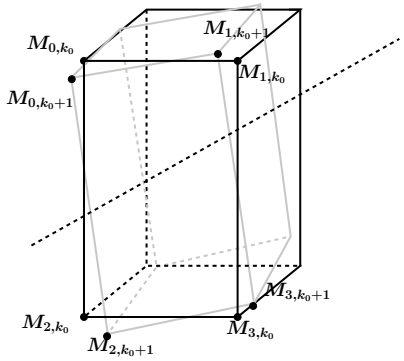

Fig. 5. Ill-posed inverse problem. Possible solutions for the $\boldsymbol{B}_{k_0}$ describe the rotation axis (dashed line).

a) Estimating motion parameters: To perform our estimations , we assume that $\boldsymbol{R}$ and $\boldsymbol{V}$ are constant within the time window corresponding to our point-cloud sequence. This is compatible with the physical assumptions underlying our forward model.

Estimating the rotation of a given sequence of point clouds has been extensively studied [5] and applied in various fields. We implemented the SVD-based algorithm of K. Arun et al. [6], which allows to estimate, for each pair of consecutive frames, a rotation matrix. The matrices are then averaged [7]. As for the translational velocity, once again, an indetermination appears. Indeed, if we try to eliminate $\boldsymbol{B}_k$ from (2) by expressing $\dot{\boldsymbol{M}}_{i,k+1} = \boldsymbol{M}_{i,k+2} - \boldsymbol{M}_{i,k+1}$ as a function of $\boldsymbol{R}_k$ and $\boldsymbol{V}_k$, and replacing $\boldsymbol{R}_k$ by its estimate, we notice that the set of solutions corresponds to the plane that fits the several consecutive rotation axes of the point cloud. Our solution consists in replacing $\boldsymbol{B}_k$ by the centroid $\bar{\boldsymbol{M}}_k$ in equation 2, and considering τ past frames and τ future frames. We thus write the mean velocity on a window of length $N_{frames} = 2\tau + 1$ as

$$\hat{\boldsymbol{V}}_{k_0} = \sum_{i=1}^{N} \sum_{k=k_0-\tau}^{k_0+\tau} \tilde{\boldsymbol{M}}_{i,k+1} - \left(\hat{\boldsymbol{R}}_{k_0}\left(\tilde{\boldsymbol{M}}_{i,k} - \bar{\boldsymbol{M}}_k\right) + \bar{\boldsymbol{M}}_k\right)$$

It can be shown that this estimator is biased but asymptotically unbiased and consistent, i.e. $\hat{\boldsymbol{V}}_{k_0} \rightarrow \boldsymbol{V}_{k_0}$ and $E[(\hat{\boldsymbol{V}}_{k_0} - \boldsymbol{V}_{k_0})^2] \rightarrow 0$ as $\tau \rightarrow \infty$. Those properties are verified in the simulation section.

b) Least-squares optimization for the CoM: The estimated CoM is now constrained on the symmetry plane. Let $\boldsymbol{P}_{k_0}$ be a point on the symmetry plane and $\boldsymbol{u}, \boldsymbol{v} \in \mathbb{R}^3$ two non-colinear vectors, we write:

$$\boldsymbol{B}_{k_0,\lambda,\mu=}\boldsymbol{P}_{k_0} + \lambda\boldsymbol{u} + \mu\boldsymbol{v} \quad \lambda, \mu \in \mathbb{R}$$

The CoM can now be estimated by solving eq. 2 in the least-square sense using τ future and past frames, i.e. on a window of length $2\tau + 1$. Expressing eq. 2 for a delay τ, the CoM at time k_0 is given by:

$$\hat{\boldsymbol{B}}_{k_0,\lambda,\mu} = \arg\min_{\lambda,\mu} \sum_{i} \sum_{k=k_0-\tau}^{k_0+\tau} \left\| \left(\boldsymbol{I_3} - \hat{\boldsymbol{R}}_{k_0}^{k-k_0}\right)\boldsymbol{B}_{k_0,\lambda,\mu} - \left[\tilde{\boldsymbol{M}}_{i,k} - \left(\hat{\boldsymbol{R}}_{k_0}^{k-k_0}\tilde{\boldsymbol{M}}_{i,k_0} + (k-k_0)\hat{\boldsymbol{V}}_{k_0}\right)\right] \right\|^2$$

IV. Results

A. Simulations

The performance of the motion-based method is now evaluated through simulation. Based on a set of experimental data, typical values of parameters $\boldsymbol{V}$ and $\boldsymbol{R}$ are chosen. The space coordinates of the box-like object of figure 3 are generated using its actual dimensions. The moving point-cloud is then obtained by applying the forward model at a frame rate of $5fps$. Uniform noise is then added. For different number of frames, 200 runs are generated to assess the robustness of the estimator with respect to noise. The reconstruction error $\epsilon = \left\|\hat{\boldsymbol{B}}_{k_0} - \boldsymbol{B}_{k_0}\right\|$ is computed along with the mean and standard deviation.

Figure 6 shows how the mean of the CoM reconstruction error, i.e. the bias arising from the translational velocity estimation decreases linearly as the number of frames increases. The mean error then stabilizes, reflecting that the translational velocity estimator disposed of enough frames to correctly describe the translation. The residual error is due to the symmetry plane being defined by noisy points, which, by definition, is independent on the motion and the number of frames.

Figure 7 shows how the CoM-to-Centroid distance affects the reconstruction for different values of N_{frames}. Because the translational velocity estimator relies on rotated centroids,

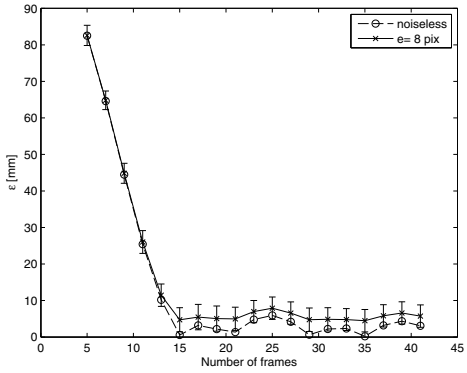

Fig. 6. ϵ vs. N_{frames}. Uniform noise equivalent to 8 pixel detection error and noiseless case.

decreasing that distance brings the centroids closer to the actual CoM, thus, the estimated CoM is closer to the true value.

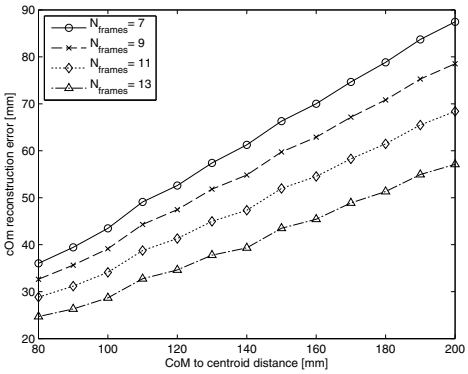

Fig. 7. ϵ vs. CoM-to-Centroid distance. Uniform noise: 8 pixels.

B. Experimental results

It is important to realize that in parabolic flights, the airplane is subject to residual accelerations during the "zero-g" phase, which is not taken into account in our model. From the acceleration signal of the airplane made available to us by the aircraft operator, a measure of the similarity of the experimental conditions with "perfect" conditions is proposed. Let G_x, G_y and G_z be respectively the x, y and z acceleration of the airplane during the sequence, expressed in the airplane's reference system. The similarity criteria, called residual acceleration is given by:

$$\boldsymbol{a}_r = \left\| \begin{array}{c} E\left[|G_x(k_0-\tau)\dots G_x(k_0+\tau)|\right] \\ E\left[|G_y(k_0-\tau)\dots G_y(k_0+\tau)|\right] \\ E\left[|G_z(k_0-\tau)\dots G_z(k_0+\tau)|\right] \end{array} \right\|$$

Table I shows the reconstruction error obtained during 5 parabolas along with the number of frames N_{frames}.

TABLE I
EXPERIMENTAL RESULTS

N_{frames}	$\boldsymbol{a}_r$ [mG]	ϵ [mm]
5	42.5	54.29
7	40	16.37
9	29.5	33
9	28.7	76
11	40	22.9

V. CONCLUSIONS

Because of important residual accelerations occurring during parabolas, only short sequences were considered such that conditions are as close as possible to an inertial reference system. Our motion-based model could be improved to account for those accelerations, thus allowing longer sequences and smaller reconstruction errors. Among the 5 parabolas dedicated to the experiment, 5 sequences of 5 to 11 frames (1-2 seconds) have been retained. The corresponding errors (16.37 to 76 mm) are indeed similar to what has been predicted via simulation (26 to 82 mm).

The simulations also suggest that to improve the accuracy, the centroid should be taken close to the actual CoM. A good a priori could be obtained in 1-g, in two different ways: Through a biomechanical modeling approach based on body segment kinematics or with a force plate based apparatus[8]. This a priori would be exploited to determine appropriate placement of fiducial markers on the subject.

ACKNOWLEDGMENT

We acknowledge the support from ESA and NOVESPACE for the organization of the 57th-ESA parabolic flight campaign. This work was supported by the Belgian Federal Science Policy Office (BELSPO), via the European Space Agency PRODEX program.

REFERENCES

[1] G. K. Prisk, S. Verhaeghe, D. Padeken, H. Hamacher, and M. Paiva, "Three-dimensional ballistocardiography and respiratory motion in sustained microgravity." pp. 1067–1074, 2001.

[2] W. E. Thornton, W. Hoffler, and Rummel, "Anthropometric changes and fluid shifts," in *Biomedical Results from Skylab*, ser. NASA Special Publication, R. S. Johnston and L. F. Dietlein, Eds., vol. 377, 1977, p. 330.

[3] B. Atcheson, F. Heide, and W. Heidrich, "Caltag: High precision fiducial markers for camera calibration." in *VMV*, R. Koch, A. Kolb, and C. Rezk-Salama, Eds. Eurographics Association, 2010, pp. 41–48.

[4] Z. Zhang, "A flexible new technique for camera calibration," vol. 22, no. 11, pp. 1330–1334, nov 2000.

[5] T. Huang and A. Netravali, "Motion and structure from feature correspondences: A review," *Proceeding of the IEEE*, vol. 82, no. 2, pp. 252–268, 1994.

[6] K. Arun, T. Huang, and S. Blostein, "Least-squares fitting of two 3-d point sets," vol. 9, no. 5, pp. 698–700, Nov. 1987.

[7] M. Moakher, "Means and averaging in the group of rotations," *SIAM J. Matrix Anal. Appl.*, vol. 24, no. 1, pp. 1–16, Jan. 2002.

[8] C. Casellato, M. Tagliabue, A. Pedrocchi, C. Papaxanthis, G. Ferrigno, and T. Pozzo, "Reaching while standing in weightlessness: a new postural solution to oversimplify movement control," *Experimental Brain Research*, vol. 216, no. 2, pp. 203–215, 2011.